0026-895X/07/7205-1280–1288$20.00
MOLECULAR PHARMACOLOGY
Copyright © 2007 The American Society for Pharmacology and Experimental Therapeutics
Mol Pharmacol 72:1280–1288, 2007

Vol. 72, No. 5
36178/3265252
Printed in U.S.A.

Polymorphic Variants of CYP2C9: Mechanisms Involved in Reduced Catalytic Activity

Lian Wei,[1] Charles W. Locuson,[2] and Timothy S. Tracy

Department of Experimental and Clinical Pharmacology, University of Minnesota, Minneapolis, Minnesota

Received March 20, 2007; accepted August 7, 2007

ABSTRACT

CYP2C9 catalyzes the demethylation of the biphasic kinetics substrate (*S*)-naproxen, and the CYP2C9*2 (R144C) and CYP2C9*3 (I359L) variants are associated with lower rates of (*S*)-naproxen demethylation. To assess the reasons for these reductions in catalytic activity of the two variants and potential substrate concentration-dependent differences in a biphasic kinetics substrate, cytochrome P450 (P450) cycle coupling and uncoupling were monitored during coincubation of (*S*)-naproxen and CYP2C9 over a range of P450 reductase concentrations. Coupling was greatest in the CYP2C9.1 enzyme, followed by CYP2C9.2, and then CYP2C9.3. Uncoupling in CYP2C9.1 and CYP2C9.3 was primarily to H_2O_2. In contrast, CYP2C9.2 uncoupled to excess water preferentially. The conversion of enzyme to the high spin state was similar in CYP2C9.1 and CYP2C9.2, but lower in CYP2C9.3. It is noteworthy that neither altered substrate binding nor altered interaction with reductase seemed to be involved in reduced catalysis. These results suggest that in addition to coupling differences, differential uncoupling to shunt products and differences in spin state help explain the reduced catalytic activity in these enzymes.

The cytochrome P450 (P450) enzymes are responsible for the biotransformation of a wide range of exogenous and endogenous substrates (Wrighton and Stevens, 1992). P450-mediated metabolism occurs via a catalytic cycle (Scheme 1) that involves several steps: 1) substrate binding; 2) one-electron addition to the substrate-P450 complex by CPR; 3) oxygen binding to the ferrous P450; 4) transfer of a second electron by either CPR or cytochrome b_5 and protonation of the resulting iron-peroxo anion intermediate; 5) cleavage of the O–O bond to generate H_2O; 6, 7) oxidation of the substrate; and 8) and release of product with subsequent regeneration of ferric P450 (Schlichting et al., 2000; Ortiz de Montellano and De Voss, 2002; Groves, 2003). However, this cycle does not always result in the production of metabolic product. Three abortive reactions may occur during the catalytic cycle, resulting in the production of shunt products and returning of the P450 to its ferric state, including 1) auto-oxidation of the oxy-ferrous P450 to generate superoxide anion; 2) release of the hydroperoxo species to produce hydrogen peroxide (hydrogen peroxide may also be produced from dismutation of the superoxide anion produced in 1); and 3) four-electron reduction of dioxygen with the formation of one extra molecule of water (Gorsky et al., 1984; Loida and Sligar, 1993; Bernhardt, 1996). Together, these reactions are collectively referred to as the uncoupling of the P450 catalytic cycle.

CYP2C9 is one of the major human hepatic cytochrome P450 isoforms, and it is responsible for the metabolism of several commonly used drugs, such as (*S*)-warfarin (Rettie et al., 1992), phenytoin, tolbutamide (Veronese et al., 1991), and a number of nonsteroidal anti-inflammatory drugs (Zhao et al., 1992; Leemann et al., 1993; Rodrigues et al., 1996; Tracy et al., 1996). In addition, polymorphic variants of CYP2C9 have been identified as being expressed in several human populations. The most common (and studied) allelic variants of CYP2C9, apart from the wild-type CYP2C9.1, are CYP2C9.2 (R144C) and CYP2C9.3 (I359L), which are most commonly observed in the white population and exhibit reduced metabolism of most substrates both in vitro and in vivo (Furuya et al., 1995; Haining et al., 1996; Stubbins et al., 1996; Sullivan-Klose et al., 1996; Steward et al., 1997; Yamazaki et al., 1998; Takanashi et al., 2000; Higashi et al., 2002). Naproxen [(*S*)-6-methoxy-α-methyl-2-naphthaleneacetic acid], an nonsteroidal anti-inflammatory drug, has been widely used in the treatment of pain or inflammation, and it is marketed commercially as the (*S*)-enantiomer. The oxidative biotransformation of naproxen seems to result in the formation of a single demethylated metabolite, desmethylnaproxen (Thompson and Collins, 1973). It is noteworthy that this naproxen demethylation is mediated primarily by

This work was supported in part by grant GM069753 from the National Institutes of Health (to T.S.T.).

[1] Current affiliation: Vertex Inc., Cambridge, Massachusetts.

[2] Current affiliation: Pfizer Animal Health, Veterinary Medicine Research and Development, Metabolism and Safety, Kalamazoo, Michigan.

Article, publication date, and citation information can be found at http://molpharm.aspetjournals.org.
doi:10.1124/mol.107.036178.

ABBREVIATIONS: P450, cytochrome P450; CPR, cytochrome P450 reductase; DLPC, dilauroylphosphatidylcholine.

CYP2C9, and it exhibits biphasic atypical (non-Michaelis-Menten) kinetics, suggesting that two naproxen molecules may bind in the active site simultaneously with different kinetic properties (low K_m-low V_{max} and high K_m-high V_{max}) (Tracy et al., 1997; Korzekwa et al., 1998).

The effects of CYP2C9.1, CYP2C9.2, and CYP2C9.3 on the metabolism of (*S*)-naproxen and the resulting kinetic profiles have been reported previously (Tracy et al., 2002; Hummel et al., 2004). Biphasic kinetics have been observed with the wild-type enzyme. The CYP2C9.2 variant also exhibited biphasic kinetics but with a modest reduction in reaction velocity, whereas linear kinetics and a substantial reduction in reaction velocity were observed with the CYP2C9.3 variant over the concentration range studied. However, to date, no studies have been conducted to assess the effects of the CYP2C9 allelic variants on the P450 reaction cycle with respect to coupling and uncoupling of substrate metabolism and the role this plays in reduced reaction velocity. Furthermore, the coupling and uncoupling of a substrate such as (*S*)-naproxen that exhibits atypical kinetics due to the presumed simultaneous binding of two substrate molecules is unknown. To this end, a series of experiments were conducted with the simplest catalytically active P450 system (P450, CPR, and lipid) to assess the reaction stoichiometry of this process in CYP2C9.1, CYP2C9.2, and CYP2C9.3. The proportion of CPR to P450 was studied over a range of ratios to assess the effects of this redox partner in each of the enzymes. Furthermore, substrate-induced effects on the heme iron spin-state equilibrium were monitored to explain differences in P450 reaction cycle coupling and uncoupling.

Materials and Methods

Chemical and Reagents. Acetonitrile, potassium phosphate, and sodium hydroxide were purchased from Thermo Fisher Scientific (Waltham, MA). NADPH, dilauroylphosphatidylcholine, (*S*)-naproxen, xylenol orange sodium salt, hydrogen peroxide solution (30%), ammonium iron(II) sulfate, D-sorbitol, sulfuric acid, α-ketoglutarate, D-(*S*)-(+)-*threo*-isocitric acid monopotassium salt, isocitrate dehydrogenase, trichloroacetic acid, sodium dithionite, and aniline were obtained from Sigma-Aldrich (St. Louis, MO). 2,4-Dinitrophenylhydrazine was obtained from Spectrum Chemical (Gardena, CA). 2-Fluoro-4-biphenyl acetic acid was a gift from the former Pharmacia Co. (Kalamazoo, MI). Desmethylnaproxen was a gift from the former Syntex Laboratories (Palo Alto, CA). Recombinant human CPR was purchased from Invitrogen (Carlsbad, CA).

Enzyme Expression and Purification. The full-length human CYP2C9 and variants were expressed in *Esccherichia coli* (DH5α-F′IQ) and purified as described previously (Cheesman et al., 2003; Hummel et al., 2005). Constructs contained the full-length N-terminal membrane-binding helix, but residues 2 to 8 were mutated to a mitochondrial P450 sequence (ALLLAVF) to aid expression in *E. coli* (Barnes et al., 1991). A 6× histidine tag was added to the C terminus to facilitate purification. P450 concentration was determined using the method of Omura and Sato (1964) and an extinction coefficient of 91 mM^{-1} cm^{-1} for the reduced carbon monoxide-complexed enzyme.

Enzyme Reconstitution and Incubation Conditions. Enzyme reconstitution and incubation conditions were described previously (Tracy et al., 2002). Purified enzymes were reconstituted in dilauroylphosphatidylcholine vesicles (extruded through a 200-nm pore size membrane), with human P450 reductase (Invitrogen, Carlsbad CA) in various ratios. The quantity of enzyme used per incubation varied depending on the assay (5–20 pmol for metabolite and H_2O_2 assays and 30 pmol for NADPH assays). To determine the kinetics of the reaction, the CYP2C9 enzyme mixtures were incubated with nine concentrations

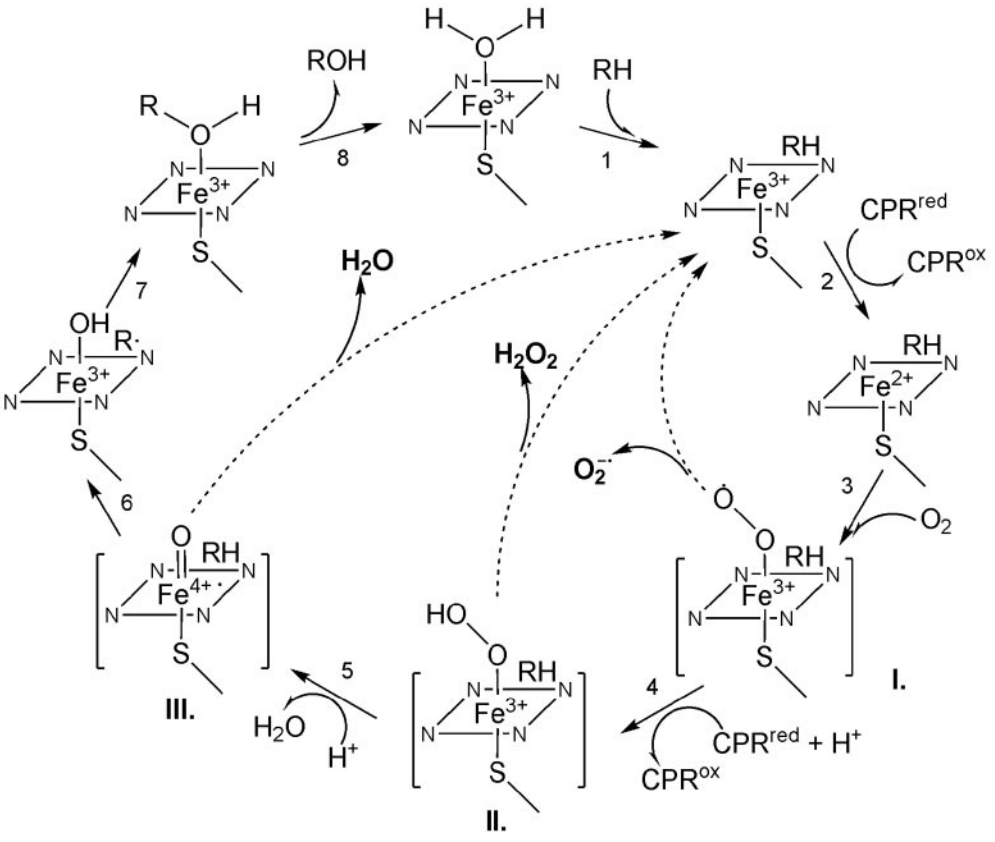

Scheme 1. Generalized P450 catalytic pathway. Fe, iron atom in P450 heme; RH, substrate; ROH, product; CPR^{ox} and CPR^{red}, oxidized and reduced states, respectively, of the P450-reductase involved in electron transfer; I, peroxo intermediate; II, hydroperoxy intermediate; III, iron-oxene intermediate.

of (*S*)-naproxen (20–2100 μM) in the presence of 50 mM potassium phosphate buffer, pH 7.4, at 37°C in a final volume of 200 μl. After a 3-min preincubation, reactions were initiated by the addition of NADPH (1 mM). After 20 min, reactions were quenched by the addition of 200 μl of acetonitrile containing 180 ng of 2-fluoro-4-biphenyl acetic acid (internal standard) and then with 40 μl of 50% (v/v) concentrated H_3PO_4. The same procedures with minor modification were used in the experiments aimed at measuring metabolite and H_2O_2 in the same reaction. In these cases, 10 pmol of P450 was incubated with various ratios (0.25–16) of human CPR and (*S*)-naproxen at a concentration of either 150 or 1500 μM for 16 min and quenched by the addition of 20 μl of acetonitrile. Aliquots (50 μl) were then removed for measurement of hydrogen peroxide (see below), whereas to the remainder, 100 μl of acetonitrile containing 480 ng of 2-fluoro-4-biphenyl acetic acid (internal standard) and 27 μl of 7.4 M H_3PO_4 were added and processed as described above for measurement of metabolite. The samples were centrifuged at 10,000*g* for 4 min, and 50 μl of supernatant was directly injected onto the high-performance liquid chromatography system. Under these conditions, metabolite formation was linear with respect to time and P450 concentration. All experiments were performed at least in duplicate.

Quantitation of Desmethylnaproxen Formation. Measurement of desmethylnaproxen formation by high-performance liquid chromatography after incubation of (*S*)-naproxen was carried out exactly as described previously (Tracy et al., 1997).

Kinetic Data Analysis. The formation of desmethylnaproxen from (*S*)-naproxen was fit to a biphasic kinetic expression using nonlinear regression:

$$v = \frac{(V_{m1} \times [S])(CL_{int} \times [S]^2)}{K_m + [S]} \quad (1)$$

or a linear equation:

$$v = CL_{int} \times [S] \quad (2)$$

All data fitting was performed with SigmaPlot 8.0 (Systat Software, Inc., Point Richmond CA), and appropriateness of the fits was determined by examination and comparison of the residuals, residual sum of squares, coefficients of determination, and *F* values.

Hydrogen Peroxide Assay. Hydrogen peroxide produced during incubations of CYP2C9 with or without (*S*)-naproxen was monitored with the xylenol orange dye method (Jiang et al., 1990). Fresh xylenol orange reagent was prepared daily from stocks of 1 M D-sorbitol, 25 mM ammonium Fe(II) sulfate in 2.5 M H_2SO_4, and 10 mM xylenol orange sodium salt. Working reagent was prepared by adding D-sorbitol (final concentration 0.1 M), xylenol orange (final concentration 125 μM), and ammonium Fe(II) sulfate (10% of total volume) sequentially to distilled water. Enzyme reactions were carried out for 16 min. At the end of the incubation, 20 μl of acetonitrile was used to stop the reaction, and a 50-μl aliquot of the mixture was added to 450 μl of freshly prepared xylenol orange reagent. Samples were allowed to stand for 45 min at room temperature, and then the absorbance was measured at 560 nm (Aminco DW2000 UV-Vis spectrophotometer with Olis upgrade; Olis Inc., Bogart, GA) after blanking the spectrophotometer with an identically prepared enzyme incubation, minus NADPH. The rate of hydrogen peroxide consumption at each CPR:P450 ratio was calculated as the difference between corresponding absorbances measured in the presence and absence of substrate, and compared with a standard curve generated with 1 to 50 μM hydrogen peroxide (assuming an extinction coefficient of 43.6 M^{-1} cm^{-1} at 240 nm).

Assay of NADPH Consumption. NADPH consumption during reaction of substrate with each of the CYP2C9 enzymes was measured spectrophotometrically based on the conversion of isocitrate to α-ketoglutarate by isocitrate dehydrogenase in the incubation mixtures and the subsequent reaction of the formed α-ketoglutarate with 2, 4-dinitrophenylhydrazine (Friedemann, 1957). Reaction conditions were optimized from previously described methods (Anthon and Barrett, 2003). The enzyme incubation reactions were allowed to proceed for 15 min at 37°C, and then they were quenched with trichloroacetic acid (20 μl of 70% solution) and centrifuged for 5 min at 10,000 rpm in a microcentrifuge. Fifty microliters of a 60 mg/100 ml solution of 2,4-dinitrophenylhydrazine was then added to 250 μl of the resulting supernatant, and the samples were placed in a 37°C water bath for 10 min. The samples were then removed, 100 μl of 5 M NaOH was added, and the absorbance at 515 nm was immediately measured on a DU 530 UV-Vis spectrophotometer (Beckman Coulter, Fullerton, CA). The spectrophotometer was blanked with a control enzyme incubation devoid of NADPH. Control incubations where substrate was absent were carried out at each CPR:P450 ratio studied and subtracted from the absorbance readings measured in the presence of substrate. Standard curves were prepared over the range of 0 to 50 nmol of α-ketoglutarate in 50 mM potassium phosphate buffer, and they were processed in the same manner as enzyme incubations.

Estimation of Excess Water Formation. Based on Scheme 1, it is assumed that part of the total consumed NADPH is used to form metabolite and H_2O_2, and the remainder is consumed to produce excess water. Because two molecules of NADPH are consumed for every one molecule of H_2O produced, the relationship is equal to 2. Thus, the following equation modified from (Fang et al., 1997) was used to estimate the rate of excess water formation:

$$H_2O = \frac{(NADPH - (Metabolite + H_2O_2))}{2} \quad (3)$$

Spectral Binding. Absolute spectra were obtained to evaluate enzyme-substrate affinity as reported previously (Kumar et al., 2006), based on the alteration in heme iron spin state that occurs when active site water(s) is displaced through (*S*)-naproxen binding. In brief, 200 pmol of enzyme and 0.5 μg/pmol DLPC in 50 mM potassium phosphate buffer, pH 7.4, were placed into the sample cuvette. The reference cuvette only contained DLPC and potassium phosphate buffer. To determine the spectral changes occurring with increasing concentrations of (*S*)-naproxen (5–1000 μM), equal volumes of stock (*S*)-naproxen were added into both the sample and reference cuvettes, and a 3-min equilibrium interval was allowed between readings. Spectral binding experiments were conducted on the Aminco DW2000 spectrophotometer described above by scanning from 340 to 500 nm. This method helps prevent the large signal of naproxen from interfering with the spectrum of the enzyme. The temperature of the cell was held constant at 30°C with a Julabo F12 compact refrigerated circulator with an external Julabo ED temperature controller (Julabo USA, Inc., Allentown, PA). The difference in absorbance between high-spin (390-nm) and low-spin (418-nm) components was calculated and plotted against (*S*)-naproxen concentration. The data were fit by nonlinear regression SigmaPlot 8.0 (Systat Software, Inc.) to estimate the spectral binding constant (K_s) from the titration binding curve using the following equation:

$$\Delta A = \frac{B_{max\,1} \times [S]}{K_{s1} + [S]} + \frac{B_{max\,2} \times [S]}{K_{s2} + [S]} \quad (4)$$

The equilibrium dissociation constant (K_d) of the CPR-CYP2C9 complex was determined by measuring the spectral change occurring when CPR is added to a solution containing 200 pmol of CYP2C9 enzyme and 0.5 μg/pmol DLPC with 50 mM potassium phosphate buffer, pH 7.4, and 20% glycerol, analogous to the method used to determine the cytochrome b_5 dissociation constant with rabbit CYP2B4 (Tamburini et al., 1985). Experiments were conducted with the spectrophotometer used for monitoring naproxen binding. The reference cuvette contained DLPC, phosphate buffer, and glycerol. CPR was titrated into both sample and reference cuvettes over the range of 0.001 to 0.9 μM, and samples scanned from 340 to500 nm to obtain the absorbance difference of the low- (418-nm) and high-spin (390-nm) Soret bands. Experiments were carried out at 30°C, and samples were equilibrated for 20 min after each addition of CPR. Because the K_d value of CPR to CYP2C9 was estimated to be much lower than the concentration of CYP2C9, and

because multiple binding events were evident, the resulting absorbance data were fit using Dynafit (Biokin, Inc., Pullman WA). The largest change in absorbance was achieved before an equimolar amount of CPR had been added to the CYP2C9 enzymes. This possibly indicates that only some of the P450 sample is available to CPR or that multiple complexes containing oligomers of P450 and/or CPR form and have different extinction coefficients. Because a second binding phase at higher CPR concentrations was observed, but the exact P450 oligomer-CPR complexes being formed are not known, the data were fit to two simple equilibria where [P450] was constant: P450 + CPR $\rightleftharpoons$ P450 × CPR and P450 × CPR + CPR $\rightleftharpoons$ CPR × P450 × CPR. These expressions are dependent on [CPR], and they do not consider different P450 oligomers or conformations, but functionally they are similar to the more probable scenario P450 + P450 × P450 + 2CPR $\rightleftharpoons$ P450 × CPR + P450 × P450 × CPR, where oligomeric state or changes in the oligomeric state are associated with distinct absorptivities. It is not clear what species exist either in vitro or in vivo, but these events can be assumed to be more complex than 1:1 binding.

Spin-State Analysis. Substrate-induced spin state changes with the three CYP2C9 enzymes were measured as described above for spectral binding measurements. Spectral titrations with (*S*)-naproxen (150 and 1500 μM final concentrations) were performed by adding equal volumes of stock (*S*)-naproxen to both sample and reference cuvettes followed by spectral scanning between 320 and 500 nm. Before scanning, the sample and reference cuvettes were allowed to equilibrate for 3 min with enzyme and substrate. Absolute spectra were then obtained to estimate the percentage of conversion of CYP2C9 from low spin to high spin using the relative low-spin peak area (Roberts et al., 2005). Deconvolution of spectra was carried out with the multiple Gaussian curve fitting available in Origin Pro, version 7.5 (OriginLab Corp., Northampton, MA). The model was developed to include three components: a low-spin component (~416–420 nm), a high-spin component (~390–405 nm), and δ-bands (~360 nm). Aniline (25 mM) was used to convert the relatively small amount of high-spin enzyme (in the absence of substrate) to the low-spin state followed by peak deconvolution. The resulting low-spin peak area was then used as the low-spin reference. The amount of low-spin heme iron is correlated to the low-spin peak areas deconvoluted from samples of different P450 concentrations (R^2 = 0.99).

Results

Desmethylnaproxen Formation. Kinetic profiles for the CYP2C9-mediated formation of desmethylnaproxen from (*S*)-naproxen are presented in Fig. 1A. Metabolism by CYP2C9.1 and CYP2C9.2 was best fit with a biphasic kinetics equation (eq. 1), whereas the formation of metabolite by CYP2C9.3 was best fit by a linear equation (eq. 2). At low substrate concentration (<200 μM), CYP2C9.1 and CYP2C9.2 produced similar metabolite formation rates, although these values diverged at substrate concentrations beyond 200 μM.

Production of desmethylnaproxen from (*S*)-naproxen (1500 μM) was evaluated over a range of CPR:P450 ratios, 0.25 to 16 (Fig. 1B). Metabolism of (*S*)-naproxen by CYP2C9.1 and its variants was also assessed at low (*S*)-naproxen concentration (150 μM) (Table 1) at a fixed CPR:P450 ratio of 2. The relative ranking of metabolite formation rates at 150 μM (*S*)-naproxen was the same as with the high concentration of (*S*)-naproxen (1500 μM). In all cases, metabolite formation increased up to a CPR:P450 ratio of either 2 or 4, and then it began to decrease with all three enzymes. Differences in metabolite formation were evident among the three enzymes, with CYP2C9.1 exhibiting the highest metabolite formation rate at each CPR:P450 ratio (CYP2C9.1 > CYP2C9.2 > CYP2C9.3) except at the very highest CPR:P450 ratios where the metabolite formation rates for CYP2C9.1 and CYP2C9.2 were essentially equivalent. In addition, CYP2C9.1 exhibited the greatest percentage of change in metabolite formation of the three enzymes (CYP2C9.1 > CYP2C9.2 > CYP2C9.3) at increasing reductase concentrations. Dialysis of glycerol from CPR did not alter these effects of CPR concentration.

Hydrogen Peroxide Formation. The degree to which P450 reaction cycle uncoupling yields H_2O_2 was evaluated at various CPR:P450 ratios at an (*S*)-naproxen concentration of 1500 μM (Fig. 2A). H_2O_2 formation rates increased up to a CPR:P450 ratio of 2 for each of the enzymes, then they decreased in all three cases at higher ratios of CPR:P450. CYP2C9.3 produced more H_2O_2 than CYP2C9.2 but less than CYP2C9.1. In the CYP2C9.2 enzyme, increasing reductase ratios had the least effect on production of H_2O_2. Using a low concentration of (*S*)-naproxen (150 μM) and a CPR:P450 ratio of 2, the relative rankings of the enzymes with respect to H_2O_2 formation (CY2C9.1 > CYP2C9.2 > CYP2C9.3) differed from that observed at higher (*S*)-naproxen concentrations (Fig. 2A; Table 1)

NADPH Consumption. To ascertain whether the amino acid changes present in the CYP2C9.2 and CYP2C9.3 enzymes affect electron transfer from CPR to P450, NADPH consumption was monitored with (*S*)-naproxen (1500 μM) and a range of CPR concentrations (Fig. 2B). The NADPH consumption rate increased up to a CPR:P450 ratio of 1, and then it decreased at higher CPR:P450 ratios in all three

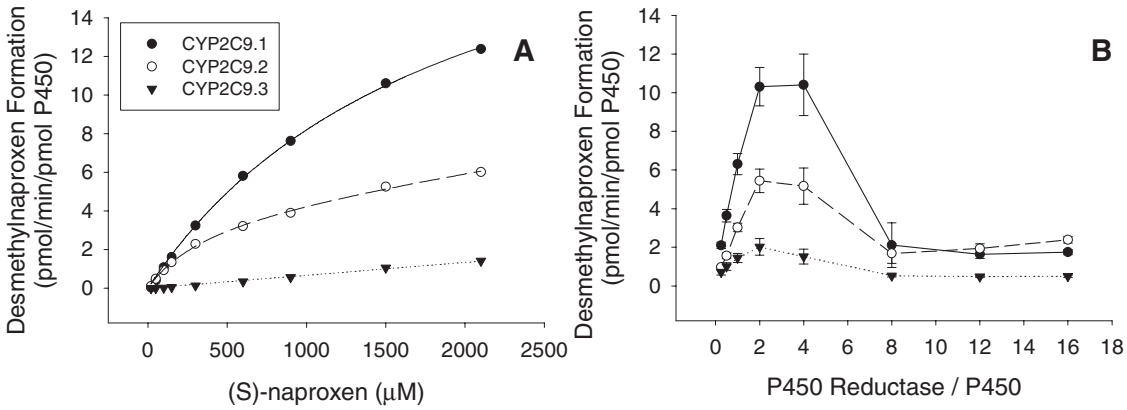

Fig. 1. (*S*)-Naproxen demethylation by CYP2C9. (A) (*S*)-Naproxen demethylation by CYP2C9.1, CYP2C9.2 and CYP2C9.3. Lines indicate the nonlinear regression fit of the data to either to eq.1 (CYP2C9.1 and CYP2C9.2) or eq.2 (CYP2C9.3). (B) Desmethylnaproxen formation by CYP2C9.1, CYP2C9.2 and CYP2C9.3 at various ratios of CPR:P450 (0.25, 0.5, 1, 2, 4, 8, 12, and 16). Each data point is the mean of triplicate determinations.

enzymes. Furthermore, CYP2C9.2 exhibited a rate of NADPH consumption similar to CYP2C9.1, although NADPH consumption was lowest with CYP2C9.3. Rankings of NADPH consumption across the enzymes at low (*S*)-naproxen concentration (150 μM) was identical to that observed at high naproxen concentrations (CYP2C9.2 > CYP2C9.1 > CYP2C9.3).

Estimates of Excess Water Formation. Excess water formation was estimated from eq. 3. Estimated excess water formation rates were higher with CYP2C9.2 compared with either of the other enzymes at all CPR:P450 ratios studied (Fig. 2C). Comparatively little excess water was formed by CYP2C9.3, and increasing reductase concentrations did not increase excess water formation substantially, as occurred with CYP2C9.1 and CYP2C9.2. Estimation of excess water was also attempted by measuring oxygen consumption with an oxygen electrode, but because of analytical sensitivity limitations, we were unable to estimate excess water formation at CPR:P450 ratios of 2 and higher with CYP2C9.1 and CYP2C9.3 at either (*S*)-naproxen concentration. For CYP2C9.2, increasing the substrate concentration resulted in increased excess water formation. However, with CYP2C9.3 the opposite occurred in that an increase in substrate concentration resulted in a decrease in excess water formation.

Effects of Different CPR:P450 Ratios on Coupling and Uncoupling. The ratio of metabolite formation:NADPH consumption, a measure of overall efficiency of coupling reducing equivalents to metabolite formation in the P450 reaction cycle, increased as the CPR:P450 ratio was raised (Fig. 3A). At each fixed CPR:P450 ratio, CYP2C9.1 exhibited the highest metabolite/NADPH ratio (CYP2C9.1 > CYP2C9.2 > CYP2C9.3), being the most coupled of the three CYP2C9 enzymes studied.

The H_2O_2 formation:NADPH consumption ratio can be used as a direct measure of uncoupling to the product H_2O_2, which can be formed either at the first or second branch points (with the assumption that superoxide formed at the first branch point dismutates to hydrogen peroxide under experimental conditions). Uncoupling to H_2O_2 increased as the CPR:P450 ratio was raised (Fig. 3B). The H_2O_2:NADPH ratio was greatest for CYP2C9.3 (CYP2C9.3 > CYP2C9.1 > CYP2C9.2). The CYP2C9 reaction cycle is least likely to uncouple to H_2O_2 with CYP2C9.2.

From Table 1, it is apparent that at the low (*S*)-naproxen concentration (150 μM), coupling (metabolite/NADPH ratio) was substantially lower in all three enzymes compared with that observed at the high concentration of substrate. At the high (*S*)-naproxen concentration (1500 μM), CYP2C9.1 coupling was approximately 4-fold, CYP2C9.2 was 2-fold, and CYP2C9.3 was 13-fold higher than observed at the low substrate concentration. For CYP2C9.1 and CYP2C9.2, uncoupling (H_2O_2/NADPH ratio) was decreased at the higher substrate concentration compared with uncoupling to H_2O_2 at the low (150 μM) substrate concentration.

Spectral Binding. To assess whether differences in (*S*)-naproxen binding exist among the three CYP2C9 enzymes, titration studies of P450 heme spectral changes against (*S*)-naproxen concentrations (Fig. 4, inset) were conducted. Plotting the difference in absorbance between 418 and 390 nm versus increasing (*S*)-naproxen concentrations yielded biphasic curves (Fig. 4), suggesting multiple binding events of (*S*)-naproxen in all three CYP2C9 enzymes. The K_s of (*S*)-naproxen with the saturable, high-affinity site of CYP2C9.1 (K_{s1} = 26.9 ± 1.3 μM) is close to that of CYP2C9.3 (K_{s1} = 30.4 ± 4.9 μM). It is noteworthy that the affinity of (*S*)-naproxen for CYP2C9.2 (K_{s1} = 8.6 ± 0.7 μM) is somewhat

TABLE 1

Comparison of CYP2C9 reaction cycle, stoichiometry, coupling, and uncoupling at both low (150 μM) and high (1500 μM) (*S*)-naproxen concentrations

Metabolite formation, H_2O_2 formation, and NADPH consumption measurements were conducted in triplicate at fixed a CPR:P450 ratio of 2. Excess H_2O values were calculated from eq. 3.

	[(*S*)-Naproxen]	Metabolite Formation	H_2O_2 Formation	NADPH Consumption	Metabolite/NADPH	H_2O_2/NADPH	Excess H_2O
	μM	*pmol/min/pmol of P450*					*pmol/min/pmol of P450*
CYP2C9.1	150	1.3 ± 0.1	13.6 ± 0.6	13.7 ± 3.0	0.09	1.0	0[a]
	1500	10.3 ± 1.0	21.2 ± 2.0	24.8 ± 2.0	0.42	0.85	0[a]
CYP2C9.2	150	1.3 ± 0.01	9.0 ± 0.7	16.1 ± 3.1	0.08	0.56	2.9
	1500	5.4 ± 0.6	11.4 ± 0.6	30.3 ± 3.7	0.18	0.38	6.7
CYP2C9.3	150	0.06 ± 0.01	4.4 ± 0.2	8.7 ± 3.2	0.01	0.51	2.1
	1500	2.0 ± 0.4	17.5 ± 2.0	15.2 ± 4.5	0.13	1.2	0*

[a] Not accurately estimable because of analytical sensitivity limitations.

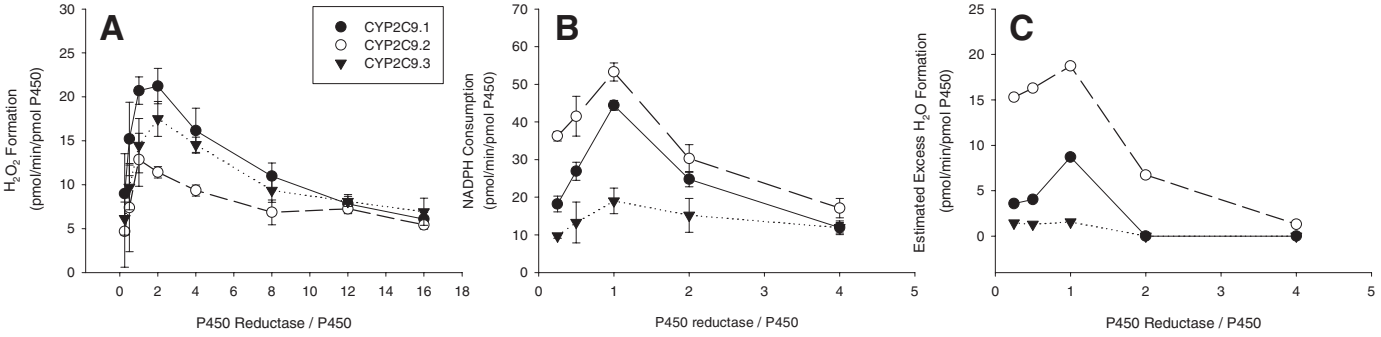

Fig. 2. Effect of CPR:P450 ratio on CYP2C9 stoichiometry in the presence of 1500 μM (*S*)-naproxen. A, H_2O_2 formation; data points represent the mean (n = 3). B, NADPH consumption; data points represent the mean (n = 3). C, estimates of excess H_2O formation rates.

greater than with the other two enzymes. K_s values for the unsaturable, low-affinity (*S*)-naproxen binding site could not be determined accurately because the estimated K_s values (>10 mM) are greater than (*S*)-naproxen solubility in phosphate buffer. Characterization of CPR binding with the three CYP2C9 enzymes was also studied by assessing the ability of CPR to affect the heme iron spin state. K_d values of the first binding event of CPR with the three CYP2C9 enzymes (Fig. 5) were also determined ($K_{d,\ 2C9.1}$ = 2.3 ± 1.0 nM; $K_{d,\ 2C9.2}$ = 1.1 ± 0.4 nM; and $K_{d,\ 2C9.3}$ = 1.7 ± 0.7 nM). These values are virtually indistinguishable suggesting that CPR interacts with all three CYP2C9 enzymes with equal affinity.

Spin-State Changes in CYP2C9 Enzymes upon (*S*)-Naproxen Binding. The percentage of each of the CYP2C9 enzymes existing in the low and high spin states was determined at both low (150 μM) and high (1500 μM) (*S*)-naproxen concentrations. The conversion of CYP2C9.1 low spin species to the high spin form is essentially the same as measured from CYP2C9.2, regardless of (*S*)-naproxen concentration (Table 2). Substrate binding introduced less spin conversion in CYP2C9.3. Conversion of CYP2C9.3 to the high-spin species was roughly half that observed with other enzymes when incubated with (*S*)-naproxen, although increasing (*S*)-naproxen concentration did increase the fraction of high-spin species.

Discussion

Genetic variation in drug-metabolizing enzymes can have profound effects on the catalytic activity of P450s, as has been observed with CYP2C9.2 and CYP2C9.3 (Yamazaki et al., 1998; Tracy et al., 2002; Iida et al., 2004). However, little is known regarding the mechanism(s) responsible for these changes in activity. The CYP2C9*2 mutation (R144C) alters

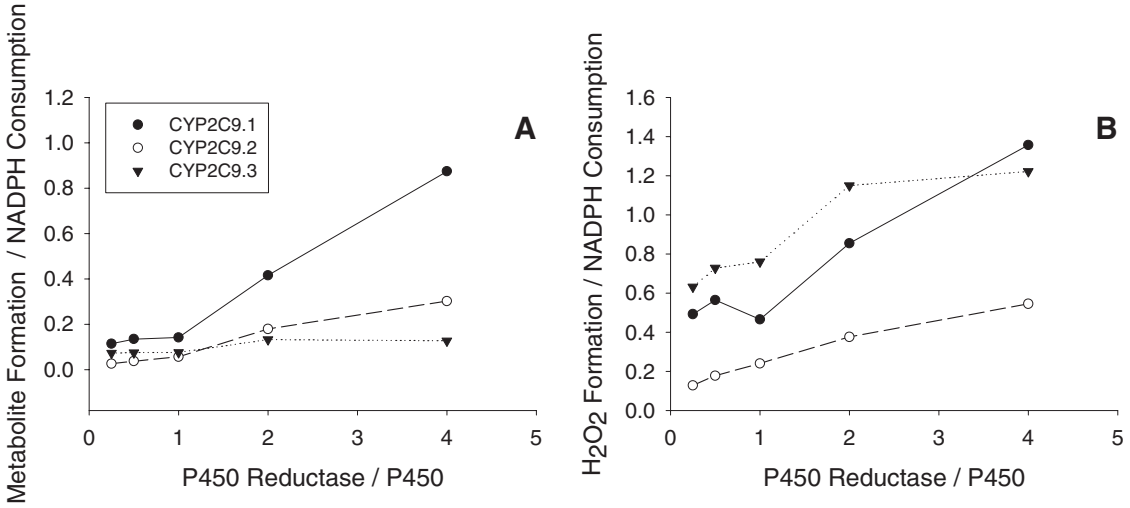

Fig. 3. Effect of various CPR:P450 ratios on CYP2C9 coupling efficiency in the presence of 1500 μM (*S*)-naproxen. A, overall coupling to product (desmethylnaproxen formation). B, uncoupling at first or second branch point (H_2O_2 formation).

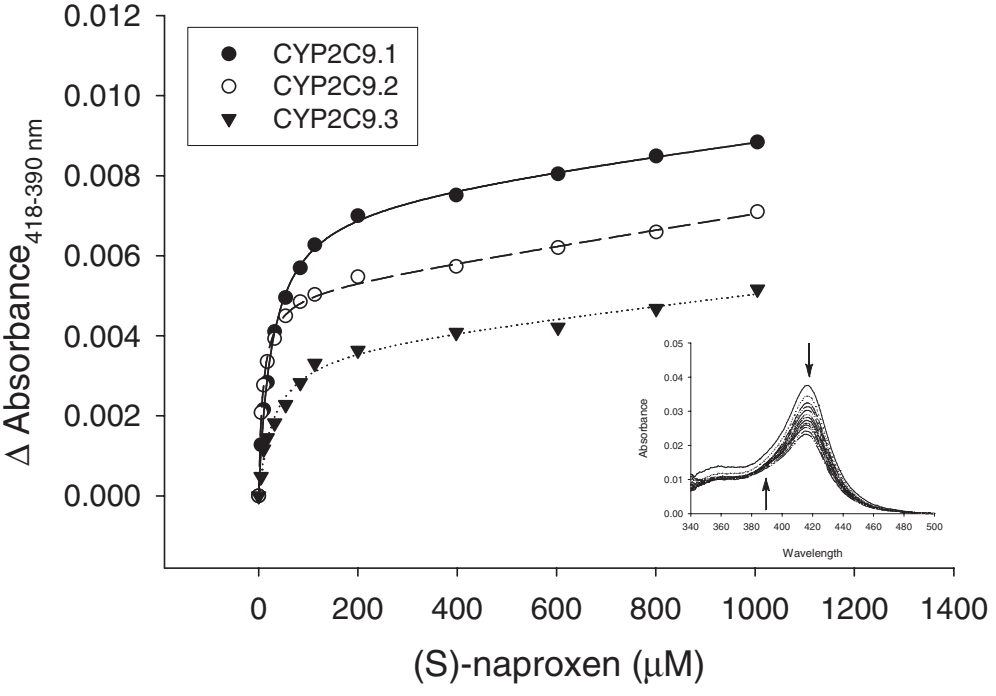

Fig. 4. Optical analysis of the (*S*)-naproxen binding equilibrium. ●, CYP2C9.1 (K_{s1} = 26.89 ± 1.32 μM); ○, CYP2C9.2 (K_{s1} = 8.55 ± 0.65 μM); and ▼, CYP2C9.3 (K_{s1} = 30.35 ± 4.92 μM). Inset, representative absolute spectra of (*S*)-naproxen incubated with CYP2C9.1.

an amino acid on the outer surface of the enzyme, whereas the CYP2C9.3 enzyme results from a conservative, single amino acid change (I359L) on the interior of the enzyme. However, crystallography studies (Wester et al., 2004) suggest that the I359L substitution is not likely to be directly involved in substrate binding, implying that a mechanism other than alterations in substrate binding may be responsible for the decrease in catalytic activity. To this end, a series of investigations were undertaken to better understand the mechanism(s) responsible for altered catalytic activity with CYP2C9.2 and CYP2C9.3.

CYP2C9 polymorphisms altered coupling efficiency (metabolite:NADPH ratio) in the presence of the substrate (*S*)-naproxen. Both variants, CYP2C9.2 and CYP2C9.3, exhibited decreased coupling efficiency. Because (*S*)-naproxen demethylation exhibits a biphasic kinetic profile, concentrations of 150 and 1500 μM thought to approach the V_{max} of each of the respective kinetic phases (low K_m-low V_{max} and high K_m-high V_{max}, respectively) were used to evaluate the effect of substrate concentration on coupling efficiency. When comparing results at the lower (150 μM) (*S*)-naproxen concentration to the higher (1500 μM) concentration, CYP2C9.3 exhibited the greatest increase in coupling (~13-fold) when substrate concentration was increased.

It has been reported that substrate binding triggers the first electron transfer to the P450 heme iron, serving to initiate the P450 catalytic cycle (Sligar and Gunsalus, 1976). In evaluating the NADPH consumption data, it seems that CYP2C9.2 triggers slightly more P450 catalytic cycles per unit time than the other two variants, but it is less productive with respect to desmethylnaproxen formation. Crespi and Miller (1997) have proposed that the R144C change in CYP2C9.2 reduces substrate metabolism through effects on the interaction of P450 with CPR, because this amino acid is located outside the active site, near the outer surface of the protein. If this were the case, one would not expect the CYP2C9.2 protein to exhibit comparable NADPH consumption rates, and likewise, the metabolite formation rate should be diminished at all substrate concentrations compared with wild-type enzyme (see above) and not just at higher substrate concentrations. The similar K_d values for the CYP2C9-CPR complex observed with CYP2C9.1 and CYP2C9.2 further supports the notion that altered reductase interactions are not responsible for the diminished substrate turnover observed with CYP2C9.2. It is of note that the binding of CPR to P450 seemed to be biphasic. This finding combined with the estimated K_d value for CPR with either enzyme being lower than the enzyme concentration present in the experimental matrix suggests that binding of CPR to both individual P450 molecules and P450 oligomer complexes may occur, resulting in the biphasic binding results noted (Hazai et al., 2005).

Increasing CPR concentrations improved coupling efficiency to different extents in each of the three enzymes. The CPR concentration that results in optimal rates for metabolite formation and NADPH consumption will be dependent on the conditions of reconstitution, but CPR was not saturating at P450:CPR ratios (e.g., 1:2) typically used for in vitro studies. Furthermore, it is proposed that the decrease in metabolite formation and NADPH consumption rates at higher CPR:P450 ratios may be due to differences in the rate of P450 reduction. Other investigators have suggested that multiple reduction states of CPR could be involved in P450 reduction (Oprian et al., 1979; Oprian and Coon, 1982). This is further supported by work with CYP2B4 by Reed and Hollenberg (2003) who demonstrated that with binding of certain substrates, the conformation of P450 does not allow CPR to bind in an orientation that allows for optimal reduction to occur (even in the presence of excess reductase), thus giving rise to the multiphasic presteady-state reduction of P450. Given that metabolite formation rate decreased at higher CPR:P450 ratios, it is tempting to speculate as to an "inhibitory"

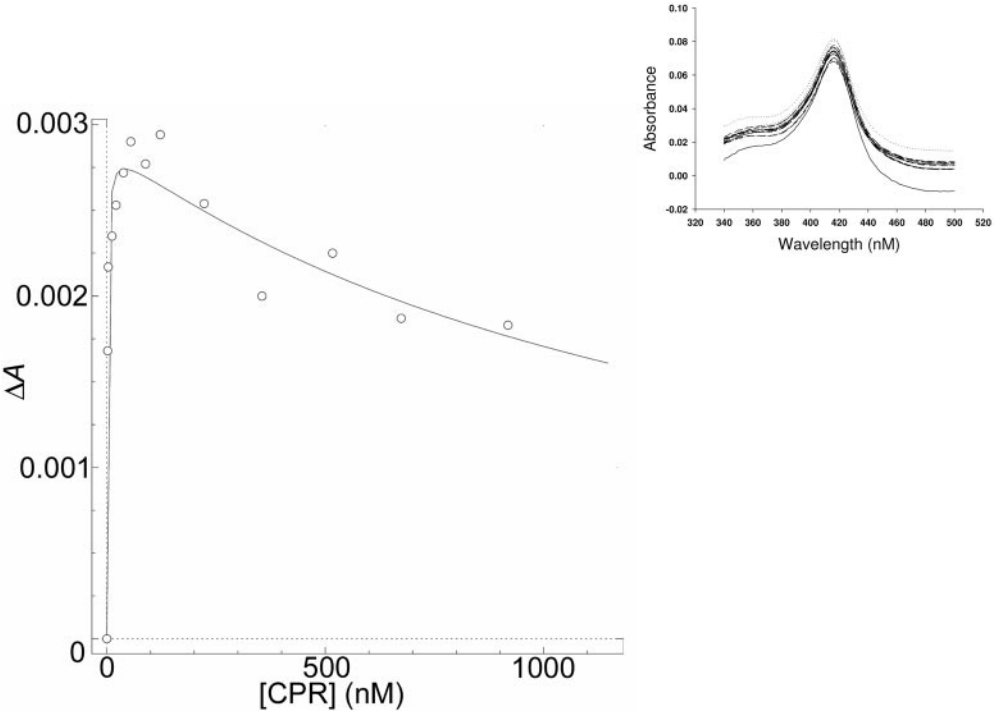

Fig. 5. Binding of CPR to CYP2C9.1. Measured by the absorbance difference between the high-spin (418-nm) and low-spin (390-nm) heme iron components in P450 absolute spectra. Inset, absolute spectra from which binding constants were derived.

effect of CPR at higher concentrations. However, it should be noted that although metabolite formation rate decreased with increasing CPR (Fig. 1B), the efficiency of the reaction cycle actually continued to increase with increasing CPR concentrations (Fig. 3, A and B) due to the even more pronounced decrease in NADPH consumption rate. Thus, the effects of higher CPR concentrations are complex and multifaceted. To ensure that this inhibition of metabolite formation at higher CPR concentrations was not due to components in the CPR enzyme buffer (after purification), glycerol and glutathione were dialyzed away, and the rates were studied again. No differences were noted, suggesting that the observed effects are due to some undefined effects of CPR and not to components of the preparation (data not shown).

The H_2O_2 shunt is considered to be one of the abortive reactions in the P450 catalytic cycle. In the presence of 1500 μM (*S*)-naproxen, CYP2C9.3 was the most uncoupled to H_2O_2, whereas CYP2C9.2 was the least uncoupled (Fig. 3B). In contrast, at lower substrate concentrations (150 μM) uncoupling to H_2O_2 was highest for CYP2C9.1. Conversely, when one examines excess H_2O formation (another uncoupling product), CYP2C9.2 exhibited both the highest amount of excess H_2O formation, irrespective of substrate concentration and the greatest increase in excess H_2O formation as the substrate concentration was increased. These results suggest that the amino acid change in CYP2C9.2 in some way results in the iron-oxene intermediate (Scheme 1) being more susceptible to breakdown to H_2O than is the case with the other enzymes and that breakdown to this product is more likely than to other shunt products (i.e., superoxide and H_2O_2). That metabolite formation rates are similar for CYP2C9.1 and CYP2C9.2 at lower (<200 μM) (*S*)-naproxen concentrations, but they diverge at higher substrate concentrations, suggesting that binding of a second substrate molecule may play a role in this increased shunting. The decreased excess H_2O formation with CYP2C9.3 in the presence of high substrate concentration suggests the P450 reaction cycle falls apart in the steps between H_2O_2 and excess H_2O production. This increase in H_2O_2 production by CYP2C9.3 at higher substrate concentrations is also related to the increased cycle triggering as suggested by the corresponding increase in NADPH consumption.

Some earlier studies suggested that the heme iron spin state may serve as a surrogate marker (Sligar et al., 1979; Tamburini et al., 1984; Backes et al., 1985). Although not applicable for every P450 isoform (Eyer and Backes, 1992) as a result of differences in reduction potentials (Ost et al., 2003), CYP2C9 is reduced much faster in the presence of substrate even though the substrate oxidation rate may be slow (Guengerich and Johnson, 1997). The current results suggest that at low (*S*)-naproxen concentrations, fractional conversion to the high spin state is consistent with the kinetic data. At low (*S*)-naproxen concentrations, both CYP2C9.1 and CYP2C9.2 exhibit similar percentages of high-spin enzyme as well as metabolite formation rates, whereas both percentage of high-spin enzyme and metabolite formation are substantially lower for CYP2C9.3 (~6.5% high spin). With higher (*S*)-naproxen concentrations (1500 μM), despite similar percentages of high-spin enzyme, lower metabolite formation rate observed with the CYP2C9.2 enzyme. Yet, this difference was accounted for with the substantially greater formation of shunt products because the defect in the catalytic cycle with CYP2C9.2 is somewhere after the initial triggering. The low fraction of high-spin enzyme observed with CYP2C9.3 is notable. The ~2-fold increase in percentage of high-spin enzyme with increasing (*S*)-naproxen concentrations, although still remaining low [~11.8% high spin at 1500 μM (*S*)-naproxen], is associated with a 35-fold increase in metabolite formation and a 5-fold increase in H_2O_2 formation, suggesting differential effects of increasing substrate on coupling and uncoupling with CYP2C9.3. Sligar and associates have recently described similar findings (Denisov et al., 2007). As more than 1 mole of ligand binds to CYP3A4, higher substrate concentrations increased high-spin character along with metabolite formation such that the population of low-affinity binding sites had a substantial effect on the positioning of other bound substrates poised for oxidation.

It is noteworthy that the high-affinity site K_s of (*S*)-naproxen with CYP2C9.1 and CYP2C9.3 was similar for these two enzymes (Fig. 4). This suggests that factors other than substrate binding and electron transfer (vide supra), such as alterations in the P450 catalytic cycle after cycle initiation, are responsible for the difference in coupling to product in CYP2C9.3 compared with the wild-type enzyme. Naganos and Poulos (2005) have proposed that a threonine (Thr252 in P450cam) widely conserved in P450s is required to stabilize the hydroperoxy intermediate (Scheme 1), favoring addition of the second proton over peroxide release, in addition to it delivering catalytic waters for dioxygen activation. In the present case, lack of change in substrate affinity and the finding that percentage of high-spin enzyme is substantially lower regardless of substrate concentration in CYP2C9.3 compared with CYP2C9.1 is consistent with alterations in the water network.

In summary, the CYP2C9 variants CYP2C9.1, CYP2C9.2, and CYP2C9.3 exhibit different degrees of coupling and uncoupling at differing concentrations of the redox partner CPR and substrate (*S*)-naproxen. Results suggest that alterations in the P450 catalytic cycle are responsible for CYP2C9.2 diminished metabolite formation rate, not alterations in CPR binding or electron transfer, as suggested previously. Destabilization of the iron-oxene complex seems to be responsible for the altered substrate turnover noted with CYP2C9.2. In the CYP2C9.3 variant, the percentage of high-spin enzyme present after substrate binding is very low compared with CYP2C9.1, despite similar substrate binding affinities, suggesting a disruption of the water network in the CYP2C9.3 variant. In addition, with CYP2C9.3, the P450 cycle seems to fall apart before formation of the iron-oxene complex. Despite only a 2-fold increase in high-spin enzyme when using higher substrate concentrations, desmethylnaproxen formation and

TABLE 2

Comparison of spin-state fraction at different (*S*)-naproxen concentrations

For low-spin content, data represent mean of duplicate determinations. Estimated high-spin content is 100% minus the low-spin content.

	[(*S*)-Naproxen]	Low-Spin Content	Estimated High-Spin Content
	μM		%
CYP2C9.1	150	84.4	15.6
	1500	77.3	22.7
CYP2C9.2	150	79.8	20.2
	1500	75.0	25.0
CYP2C9.3	150	93.5	6.5
	1500	88.2	11.8

H_2O_2 formation increase disproportionately, suggesting that binding of the second naproxen molecule improves positioning of the first-bound naproxen, thereby leading to more efficient oxidation in the CYP2C9.3 enzyme. Thus, in the CYP2C9.2 and 2C9.3 variants, amino acid substitutions arguably not involved directly in substrate binding destabilize or reduce formation of the iron-oxene complex, thereby resulting in reduced catalytic activity.

References

Anthon GE and Barrett DM (2003) Modified method for the determination of pyruvic acid with dinitrophenylhydrazine in the assessment of onion pungency. *J Sci Food Agric* **83:**1210–1213.

Backes WL, Tamburini PP, Jansson I, Gibson GG, Sligar SG, and Schenkman JB (1985) Kinetics of cytochrome P-450 reduction: evidence for faster reduction of the high-spin ferric state. *Biochemistry* **24:**5130–5136.

Barnes HJ, Arlotto MP, and Waterman MR (1991) Expression and enzymatic activity of recombinant cytochrome P450 17 alpha-hydroxylase in *Escherichia coli*. *Proc Natl Acad Sci U S A* **88:**5597–5601.

Bernhardt R (1996) Cytochrome P450: structure, function, and generation of reactive oxygen species. *Rev Physiol Biochem Pharmacol* **127:**137–221.

Cheesman MJ, Baer BR, Zheng YM, Gillam EM, and Rettie AE (2003) Rabbit CYP4B1 engineered for high-level expression in *Escherichia coli*: ligand stabilization and processing of the N-terminus and heme prosthetic group. *Arch Biochem Biophys* **416:**17–24.

Crespi CL and Miller VP (1997) The R144C Change in the CYP2C9*2 allele alters interaction of the cytochrome P450 with NADPH:cytochrome P450 oxidoreductase. *Pharmacogenetics* **7:**203–210.

Denisov IG, Baas BJ, Grinkova YV, and Sligar SG (2007) Cooperativity in cytochrome P450 3A4: linkages in substrate binding, spin state, uncoupling, and product formation. *J Biol Chem* **282:**7066–7076.

Eyer CS and Backes WL (1992) Relationship between the rate of reductase-cytochrome P450 complex formation and the rate of first electron transfer. *Arch Biochem Biophys* **293:**231–240.

Fang X, Kobayashi Y, and Halpert JR (1997) Stoichiometry of 7-ethoxycoumarin metabolism by cytochrome P450 2B1 wild-type and five active-site mutants. *FEBS Lett* **416:**77–80.

Friedemann TE (1957) Determination of α-keto acids. *Methods Enzymol* **3:**414–418.

Furuya H, Fernandez-Salguero P, Gregory W, Taber H, Steward A, Gonzalez FJ, and Idle JR (1995) Genetic polymorphism of CYP2C9 and its effect on warfarin maintenance dose requirement in patients undergoing anticoagulation therapy. *Pharmacogenetics* **5:**389–392.

Gorsky LD, Koop DR, and Coon MJ (1984) On the stoichiometry of the oxidase and monooxygenase reactions catalyzed by liver microsomal cytochrome P-450. Products of oxygen reduction. *J Biol Chem* **259:**6812–6817.

Groves JT (2003) The bioinorganic chemistry of iron in oxygenases and supramolecular assemblies. *Proc Natl Acad Sci U S A* **100:**3569–3574.

Guengerich FP and Johnson WW (1997) Kinetics of ferric cytochrome P450 reduction by NADPH-cytochrome P450 reductase: rapid reduction in the absence of substrate and variations among cytochrome P450 systems. *Biochemistry* **36:**14741–14750.

Haining RL, Hunter AP, Veronese ME, Trager WF, and Rettie AE (1996) Allelic variants of human cytochrome P450 2C9: baculovirus-mediated expression, purification, structural characterization, substrate stereoselectivity, and prochiral selectivity of the wild-type and I359L mutant forms. *Arch Biochem Biophys* **333:**447–458.

Hazai E, Bikadi Z, Simonyi M, and Kupfer D (2005) Association of cytochrome P450 enzymes is a determining factor in their catalytic activity. *J Comput Aided Mol Des* **19:**271–285.

Higashi MK, Veenstra DL, Kondo LM, Wittkowsky AK, Srinouanprachanh SL, Farin FM, and Rettie AE (2002) Association between CYP2C9 genetic variants and anticoagulation-related outcomes during warfarin therapy. *JAMA* **287:**1690–1698.

Hummel MA, Dickmann LJ, Rettie AE, Haining RL, and Tracy TS (2004) Differential activation of CYP2C9 variants by dapsone. *Biochem Pharmacol* **67:**1831–1841.

Hummel MA, Locuson CW, Gannett PM, Rock DA, Mosher CM, Rettie AE, and Tracy TS (2005) CYP2C9 genotype-dependent effects on in vitro drug-drug interactions: switching of benzbromarone effect from inhibition to activation in the CYP2C9.3 variant. *Mol Pharmacol* **68:**644–651.

Iida I, Miyata A, Arai M, Hirota M, Akimoto M, Higuchi S, Kobayashi K, and Chiba K (2004) Catalytic roles of CYP2C9 and its variants (CYP2C9*2 and CYP2C9*3) in lornoxicam 5′-hydroxylation. *Drug Metab Dispos* **32:**7–9.

Jiang ZY, Woollard AC, and Wolff SP (1990) Hydrogen peroxide production during experimental protein glycation. *FEBS Lett* **268:**69–71.

Korzekwa KR, Krishnamachary N, Shou M, Ogai A, Parise RA, Rettie AE, Gonzalez FJ, and Tracy TS (1998) Evaluation of atypical cytochrome P450 kinetics with two-substrate models: evidence that multiple substrates can simultaneously bind to cytochrome P450 active sites. *Biochemistry* **37:**4137–4147.

Kumar V, Locuson CW, Sham Y, and Tracy TS (2006) Amiodarone-analog dependent effects on CYP2C9-mediated metabolism and kinetic profiles. *Drug Metab Dispos* **34:**1688–1696.

Leemann T, Transon C, and Dayer P (1993) Cytochrome P450TB (CYP2C): a major monooxygenase catalyzing diclofenac 4′-hydroxylation in human liver. *Life Sci* **52:**29–34.

Loida PJ and Sligar SG (1993) Molecular recognition in cytochrome P-450: mechanism for the control of uncoupling reactions. *Biochemistry* **32:**11530–11538.

Nagano S and Poulos TL (2005) Crystallographic study on the dioxygen complex of wild-type and mutant cytochrome P450cam. Implications for the dioxygen activation mechanism. *J Biol Chem* **280:**31659–31663.

Omura T and Sato R (1964) The carbon monoxide-binding pigment of liver microsomes. I. Evidence for its hemoprotein nature. *J Biol Chem* **239:**2370–2378.

Oprian DD and Coon MJ (1982) Oxidation-reduction states of FMN and FAD in NADPH-cytochrome P-450 reductase during reduction by NADPH. *J Biol Chem* **257:**8935–8944.

Oprian DD, Vatsis KP, and Coon MJ (1979) Kinetics of reduction of cytochrome P-450LM4 in a reconstituted liver microsomal enzyme system. *J Biol Chem* **254:**8895–8902.

Ortiz de Montellano PR and De Voss JJ (2002) Oxidizing species in the mechanism of cytochrome P450. *Nat Prod Rep* **19:**477–493.

Ost TW, Clark J, Mowat CG, Miles CS, Walkinshaw MD, Reid GA, Chapman SK, and Daff S (2003) Oxygen activation and electron transfer in flavocytochrome P450 BM3. *J Am Chem Soc* **125:**15010–15020.

Reed JR and Hollenberg PF (2003) New perspectives on the conformational equilibrium regulating multi-phasic reduction of cytochrome P450 2B4 by cytochrome P450 reductase. *J Inorg Biochem* **97:**276–286.

Rettie AE, Korzekwa KR, Kunze KL, Lawrence RF, Eddy AC, Aoyama T, Gelboin HV, Gonzalez FJ, and Trager WF (1992) Hydroxylation of warfarin by human CDNA-expressed cytochrome P-450: a role for P-4502C9 in the etiology of (S)-warfarin-drug interactions. *Chem Res Toxicol* **5:**54–59.

Roberts AG, Campbell AP, and Atkins WM (2005) The thermodynamic landscape of testosterone binding to cytochrome P450 3A4: ligand binding and spin state equilibria. *Biochemistry* **44:**1353–1366.

Rodrigues AD, Kukulka MJ, Roberts EM, Ouellet D, and Rodgers TR (1996) [*O*-methyl ^{14}C]Naproxen *O*-demethylase activity in human liver microsomes: evidence for the involvement of cytochrome P4501A2 and P4502C9/10. *Drug Metab Dispos* **24:**126–136.

Schlichting I, Berendzen J, Chu K, Stock AM, Maves SA, Benson DE, Sweet RM, Ringe D, Petsko GA, and Sligar SG (2000) The catalytic pathway of cytochrome P450cam at atomic resolution. *Science* **287:**1615–1622.

Sligar SG, Cinti DL, Gibson GG, and Schenkman JB (1979) Spin state control of the hepatic cytochrome P450 redox potential. *Biochem Biophys Res Commun* **90:**925–932.

Sligar SG and Gunsalus IC (1976) A thermodynamic model of regulation: modulation of redox equilibria in camphor monoxygenase. *Proc Natl Acad Sci U S A* **73:**1078–1082.

Steward DJ, Haining RL, Henne KR, Davis G, Rushmore TH, Trager WF, and Rettie AE (1997) Genetic association between sensitivity to warfarin and expression of CYP2C9*3. *Pharmacogenetics* **7:**361–367.

Stubbins MJ, Harries LW, Smith G, Tarbit MH, and Wolf CR (1996) Genetic analysis of the human cytochrome P450 CYP2C9 locus. *Pharmacogenetics* **6:**429–439.

Sullivan-Klose TH, Ghanayem BI, Bell DA, Zhang ZY, Kaminsky LS, Shenfield GM, Miners JO, Birkett DJ, and Goldstein JA (1996) The role of the CYP2C9-Leu(359) allelic variant in the tolbutamide polymorphism. *Pharmacogenetics* **6:**341–349.

Takanashi K, Tainaka H, Kobayashi K, Yasumori T, Hosakawa M, and Chiba K (2000) CYP2C9 Ile359 and Leu359 variants: enzyme kinetic study with seven substrates. *Pharmacogenetics* **10:**95–104.

Tamburini PP, Gibson GG, Backes WL, Sligar SG, and Schenkman JB (1984) Reduction kinetics of purified rat liver cytochrome P-450. Evidence for a sequential reaction mechanism dependent on the hemoprotein spin state. *Biochemistry* **23:**4526–4533.

Tamburini PP, White RE, and Schenkman JB (1985) Chemical characterization of protein-protein interactions between cytochrome P-450 and cytochrome B5. *J Biol Chem* **260:**4007–4015.

Thompson GF and Collins JM (1973) Urinary metabolic profiles for choosing test animals for chronic toxicity studies: application to naproxen. *J Pharm Sci* **62:**937–941.

Tracy TS, Hutzler JM, Haining RL, Rettie AE, Hummel MA, and Dickmann LJ (2002) Polymorphic variants (CYP2C9*3 and CYP2C9*5) and the F114L active site mutation of CYP2C9: effect on atypical kinetic metabolism profiles. *Drug Metab Dispos* **30:**385–390.

Tracy TS, Marra C, Wrighton SA, Gonzalez FJ, and Korzekwa KR (1996) Studies of flurbiprofen 4′-hydroxylation. Additional evidence suggesting the sole involvement of cytochrome P450 2C9. *Biochem Pharmacol* **52:**1305–1309.

Tracy TS, Marra C, Wrighton SA, Gonzalez FJ, and Korzekwa KR (1997) Involvement of multiple cytochrome P450 isoforms in naproxen O-demethylation. *Eur J Clin Pharmacol* **52:**293–298.

Veronese ME, Mackenzie PI, Doecke CJ, McManus ME, Miners JO, and Birkett DJ (1991) Tolbutamide and phenytoin hydroxylations by CDNA-expressed human liver cytochrome P4502C9. *Biochem Biophys Res Commun* **175:**1112–1118.

Wester MR, Yano JK, Schoch GA, Yang C, Griffin KJ, Stout CD, and Johnson EF (2004) The structure of human cytochrome P450 2C9 complexed with flurbiprofen at 2.0-A resolution. *J Biol Chem* **279:**35630–35637.

Wrighton SA and Stevens JC (1992) The human hepatic cytochromes P450 involved in drug metabolism. *Crit Rev Toxicol* **22:**1–21.

Yamazaki H, Inoue K, Chiba K, Ozawa N, Kawai T, Suzuki Y, Goldstein JA, Guengerich FP, and Shimada T (1998) Comparative studies on the catalytic roles of cytochrome P450 2C9 and its Cys- and Leu-variants in the oxidation of warfarin, flurbiprofen, and diclofenac by human liver microsomes. *Biochem Pharmacol* **56:**243–251.

Zhao J, Leemann T, and Dayer P (1992) In vitro oxidation of oxicam NSAIDS by a human liver cytochrome P450. *Life Sci* **51:**575–581.

Address correspondence to: Dr. Timothy S. Tracy, Department of Experimental and Clinical Pharmacology, University of Minnesota, 308 Harvard St. SE, Minneapolis, MN 55455. E-mail: tracy017@umn.edu